

Published in final edited form as:

Microbes Infect. 2006 July ; 8(8): 2245–2253. doi:10.1016/j.micinf.2006.04.008.

Comparative investigation of the pathogenicity of three *Mycobacterium tuberculosis* mutants defective in the synthesis of *p*-hydroxybenzoic acid derivatives

Gustavo Stadthagen^a, Mary Jackson^a, Patricia Charles^a, Frédéric Boudou^a, Nathalie Barilone^a, Michel Huerre^e, Patricia Constant^d, Avraham Liav^f, Iveta Bottova^{a,1}, Jérôme Nigou^d, Thérèse Brando^d, Germain Puzo^d, Mamadou Daffé^d, Pearline Benjamin^c, Stephen Coade^c, Roger S. Buxton^c, Ricardo E. Tascon^c, Aaron Rae^b, Brian D. Robertson^b, Douglas B. Lowrie^c, Douglas B. Young^b, Brigitte Gicquel^a, and Ruth Griffin^{b,*}

^aUnité de Génétique Mycobactérienne, Institut Pasteur, Paris, France

^bCentre for Molecular Microbiology and Infection, Level 3, Flowers building, Imperial College, London, UK

^cDivision of Mycobacterial Research, MRC, National Institute for Medical Research, Mill Hill, London, UK

^dDépartement “Mécanismes Moléculaires des Infections Mycobactériennes”, Institut de Pharmacologie et de Biologie structurale, CNRS, 205, Route de Narbonne, 31077-Toulouse cedex, France

^eUnité de Recherche et d’Expertise Histotechnologie et Pathologie, Institut Pasteur, Paris

^fMycobacteria Research Laboratories, Colorado State University, Fort Collins, USA

Abstract

p-Hydroxybenzoic acid derivatives (*p*-HBADs) are glycoconjugates secreted by all *Mycobacterium tuberculosis* isolates whose contribution to pathogenicity remains to be determined. The pathogenicity of three transposon mutants of *M. tuberculosis* deficient in the biosynthesis of some or all forms of *p*-HBADs was studied. Whilst the mutants grew similarly to the wild-type strain in macrophages and C57BL/6 mice, two of the mutants induced a more severe and diffuse inflammation in the lungs. The lack of production of some or all forms of *p*-HBADs in these two mutants also correlated with an increased secretion of the pro-inflammatory cytokines tumour-necrosis factor α , interleukin 6 and interleukin 12 in vivo. We propose that the loss of production of *p*-HBADs by tubercle bacilli results in their diminished ability to suppress the pro-inflammatory response to infection and that this ultimately provokes extensive pulmonary lesions in the C57BL/6 model of tuberculosis infection.

Keywords

Mycobacterium; *Tuberculosis*; Phenolic glycolipids; *p*-Hydroxybenzoic acid derivatives

© 2006 Elsevier SAS. All rights reserved.

*Corresponding author. TB Research Group, Veterinary Laboratories Agency, Woodham Lane, New Haw, Addlestone KT15 3NB, UK. Tel.: +44 1932 341 111; fax: +44 1932 359 448. r.griffin@imperial.ac.uk (R. Griffin).

¹Present address: Department of Biochemistry, Faculty of Natural Sciences, Comenius University, Mlynska dolina CH-1, 84215 Bratislava, Slovak Republic.

1. Introduction

It is estimated that up to two billion people are infected by *Mycobacterium tuberculosis*, resulting in around eight million new cases of active disease and two million deaths every year. The development of disease after *M. tuberculosis* infection depends on the genetic background and the immune and nutritional status of the host, as well as on the nature of the infecting strain. It is becoming apparent that different strains of *M. tuberculosis* trigger different immune responses as a result of subtle differences in their cell envelope composition, and that this substantially influences their subsequent pathogenicity [1-4]. Among the principal surface ligands that directly trigger the innate inflammatory response are glycolipids, lipoglycans and lipoproteins which are recognised by a series of receptors on antigen-presenting cells, including the Toll-like receptors, the mannose receptor and DC-SIGN [5-7]. The most intensively studied mycobacterial ligand is lipoarabinomannan (LAM). Differences in the structure of the terminal sugar moieties of LAM dramatically influence the innate response triggered [8].

Recent interest has focused on phenolic glycolipids (PGL). They consist of a conserved lipid core composed of phenolphthiocerol esterified by two chains of multiple methyl-branched fatty acids (mycocerosic acids or phthioceranic acids) and a variable carbohydrate moiety which, according to the mycobacterial species, is composed of one to four *O*-methylated deoxysugars [9,10]. PGL are produced by *Mycobacterium leprae*, *Mycobacterium kansasii*, *Mycobacterium bovis*, some strains of *M. tuberculosis* and a few other slow-growing mycobacteria, including *Mycobacterium ulcerans*, *Mycobacterium marinum*, *Mycobacterium gastri*, *Mycobacterium microti* and *Mycobacterium haemophilum*. PGL-1 from *M. leprae* has been the most extensively studied phenolphthiocerol glycolipid. It has a plethora of effects on the immune system; from a role in the uptake of bacteria by Schwann cells and mononuclear phagocytes to suppressive effects on monocytic and lymphoproliferative responses [9-16]. Interestingly, many of the biological activities of PGL-1 are specifically associated with the carbohydrate moiety of this molecule.

The role of *M. tuberculosis* PGL (PGL-tb) (Fig. 1) in the pathogenesis of tuberculosis is less clear. In spite of the finding that the hypervirulence of a W-Beijing isolate of *M. tuberculosis* was associated with the presence of PGL-tb in this strain [3,17] most strains of the tubercle bacillus do not produce PGL due to a frameshift mutation in the polyketide synthase gene *pks15/1*, which is required for the assembly of the lipid moiety of the molecule [11]. However, all *M. tuberculosis* isolates analysed to date have retained the ability to produce and secrete *p*-Hydroxybenzoic acid derivatives (*p*-HBADs)-glycoconjugates which share with PGL-tb the same glycosylated aromatic nucleus [11] (Fig. 1). Since *p*-HBADs may themselves be biologically active species, as is the case with the glycosylated aromatic nucleus of PGL-1, we set out to explore the role of *p*-HBADs in the pathogenicity of *M. tuberculosis*. To this end, we used a PGL-deficient strain (with a natural frameshift in *pks15/1*) and compared the pathological and immunological behaviour of *M. tuberculosis* mutants deficient in the production of some or all forms of *p*-HBADs, derived from this strain, *in vitro* and *in vivo*.

2. Materials and methods

2.1. Bacterial strains and culture conditions

Mt103, the clinical isolate of *M. tuberculosis* used in this study and the mutants 7B7, 66C7 and 29D6 were grown in ADC-supplemented Middlebrook 7H9 medium (Difco), minimal Sauton's medium as surface pellicles or on solid, OADC-supplemented Middlebrook 7H11 medium (Difco). Where indicated, kanamycin (Kan) and hygromycin (Hyg) were added to final concentrations of 25 µg/ml and 50 µg/ml, respectively.

2.2. Screening of a *M. tuberculosis* Mt103 transposon mutant library with the monoclonal antibody CS-35

The *M. tuberculosis* Mt103 ordered transposon mutant library screened in this study is the one described earlier [18]. To rapidly identify mutants of *M. tuberculosis* with defects in LAM synthesis or transport, the anti-LAM antibody CS-35 [19] was used to detect by immuno-dot-blotting those mutants with loss of or reduced binding to the antibody. When interpreting the results, the density of culture sampled from each mutant was taken into consideration. For example, mutants that showed no reactivity and also no growth upon subculturing the library were discounted.

2.3. Identification of the transposon insertion sites

The transposon insertion site in each mutant was identified by ligation-mediated PCR [20].

2.4. Complementation studies

We previously described the complementation of mutant 66C7 [21]. The same PCR conditions and the same vector were used for the amplification, cloning and expression of *Rv2958c* and *Rv2959c* to complement 7B7 and 29D6, as were used for the complementation of 66C7. Specifically primers Rv2958c.1 (5'-ccgcgcccatatggaggaaacaaggctcgcc-3') and Rv2958c.2 (5'-gaaaggatgcatgcagacggcgcac-3'), incorporating *Nde*I and *Nsi*I restriction sites (underlined), and Rv2959c.1 (5'-cgggttaatgggctagtgtggcgactc-3') and Rv2959c.2 (5'-cccaagcttttgcggatcgagaatccgtgg-3'), incorporating *Mse*I and *Hind*III sites, were designed to amplify the entire genes, *Rv2958c* and *Rv2959c*, respectively, for direct cloning into the *Nde*I/*Pst*I and *Nde*I/*Hind*III sites of pVV16. The production of the recombinant *Rv2958c* and *Rv2959c* proteins in the complemented mutants was analysed by Western blotting with a mouse monoclonal anti-His antibody (Penta-His antibody, Qiagen).

2.5. Biochemical analyses of *M. tuberculosis* mutants

For flow cytometry analyses of whole cells, bacteria grown in 7H9 were harvested by centrifugation and washed twice with PBS containing 2% FCS (PBS-FCS). Washed cells were alternatively heat-killed or used directly for labelling. Cells were incubated in PBS-FCS containing the monoclonal antibody CS-35 for 1 h at 4 °C. Cells were then washed twice and incubated in PBS-FCS containing a rabbit anti-mouse Cy3-conjugated secondary antibody. After 1 h of incubation at 4 °C, cells were washed, resuspended in 5% PFA in PBS and analysed with a FACSCalibur™ 1506 System (Becton Dickinson).

For all other analyses, bacterial strains were grown in Sauton's medium. Lipomannan (LM) and LAM were extracted from disrupted bacterial cells by reflux in 40% aqueous ethanol at 60 °C. After centrifugation at 4000 rpm for 30 min, the extracts were filtered through 0.2 µm-pore size filters (Sarstedt), evaporated to dryness and finally resuspended in milli-Q water. LM and LAM extracted from bacterial cells were analysed by SDS-PAGE fractionation and silver staining and by Western analysis using the CS-35 Mab. The monosaccharide content of the LM and LAM extracted from bacterial cells and that of culture filtrates (containing arabinomannan, glucan and mannan) were analysed by capillary zone electrophoresis as described [22] and related to the amounts of dried cells. *p*-HBAD production was investigated by thin-layer chromatography (TLC) analysis of total lipids extracted from bacterial cells and culture media as previously described [21].

2.6. Purification and structural analysis of glycoconjugate G2

G2 was purified from the culture filtrate of the complemented strain 7B7/pVV16Rv2958c by preparative TLC using CHCl₃/CH₃OH/H₂O (90:10:1, vol:vol:vol) as the eluent. Methanolysis and trimethylsilyl (TMS) derivatization of glycoconjugate G2 were carried out

as described [21]. The TMS derivatives were solubilized in either petroleum ether, for gas chromatography (GC) and GC-mass spectrometry (GC-MS), or in chloroform for MALDI-TOF mass spectrometry. MALDI-TOF mass spectrometry, GC and GC-MS analyses were performed as described [11,21]. NMR spectra were recorded on an Avance Bruker spectrometer equipped with a 600 MHz cryoprobe and with topspin 1.3 software system. The sample was dissolved in CDCl₃ (99.96 atom % D) and analysed in 5 mm NMR tubes. ¹H spectra were recorded at 295 K; ¹H chemical shifts were expressed with respect to the internal CDCl₃ (at 7.27 ppm).

2.7. Infection of mice

6- to 8-week-old female C57BL/6 mice were infected intravenously with 10⁵ CFU of *M. tuberculosis* wild-type and mutant strains as described [23]. Five mice were used per experimental time point and per strain.

2.8. Histopathological assessment of mice lungs

For histopathology studies, four additional mice were infected in each experimental group. Lungs from killed mice were aseptically removed. The superior, median and inferior lobes of the lungs were fixed in 3.7% neutral-buffered formaldehyde for two days and embedded in paraffin (melting fusion point, 60 °C). Serial 5 µm sections were then cut and stained with hematoxylin-eosin or by the Ziehl-Neelsen procedure. Inflammatory lesions within the alveolae, bronchus wall, vessels and pleural effusions were studied. The surface of granulomas was calculated using the Leica QWin program (Leica Microsystems Imaging Solutions Ltd.). Sections were blindly evaluated by a pathologist.

2.9. Preparation and infection of murine bone marrow macrophages (BMMs)

BMMs were prepared from the femurs and tibias of 6- to 8-week-old C57BL/6 mice (CERJanvier, France) and infected as described [23]. Macrophages were seeded in 12-well plates (5 × 10⁵ cells per well) and allowed to differentiate for 7 days. All infections (MOI of 0.1 bacilli per cell) were carried out at 37 °C in a 5% CO₂ atmosphere.

2.10. Cytokine analysis

Cytokine secretion by macrophages was tested by infecting cells with *M. tuberculosis* at 10 bacilli per cell and harvesting culture supernatants 24 and 48 h after infection. The supernatants were sterile filtered and analysed for the presence of cytokines and chemokines (IL-12, IL-6, TNFα, IL-10) by cytometric bead array technology (BD Biosciences) and ELISA as described earlier [2].

3. Results

3.1. Isolation of p-HBAD mutants from a transposon library of *M. tuberculosis*

In the course of an initial investigation on LAM, we screened over 6000 transposon mutants of *M. tuberculosis* Mt103 with the monoclonal antibody CS-35 to identify mutants with altered expression of surface LAM. Twenty-five mutants showing reduced antibody binding were selected, and the insertion site of the transposon was mapped for each of these (Table 1). Unexpectedly, we found that in three of the mutants, 7B7, 29D6 and 66C7, insertions had occurred in a region of the genome associated with PGL synthesis. Specifically, the transposons were inserted 17 base pairs upstream from the start codon of the glycosyltransferase gene *Rv2958c* in 7B7, 666 bp downstream from the predicted start codon of the methyltransferase gene *Rv2959c* in 29D6 and 237 bp downstream from the start codon of the chorismate pyruvate-lyase gene *Rv2949c* in 66C7. We confirmed that the

transposon insertion abolished the expression of *Rv2958c* in 7B7 by RT-PCR (data not shown).

3.2. Biochemical analyses of the mutant strains

To further characterise the binding of the mutants to CS-35, we performed FACS analysis on each of the mutant strains. With this approach, we observed no difference in the overall binding of the mutants compared to the wild-type strain to CS-35, indicating that the mutants exposed at their surface the same amount of LAM as Mt103 (data not shown). Using different analytical methods (see Section 2.5), we then compared the LAM and LM contents as well as the monosaccharide contents of the LAM and LM fraction and culture filtrates from 7B7, 29D6, 66C7 and wild-type *M. tuberculosis* Mt103. Again, no quantitative or qualitative differences were observed. Taken together, these results show that the mutations in 7B7, 29D6 and 66C7 do not affect LAM biosynthesis. We therefore have to conclude that the transposon insertions in the mutants had some effect either on exposure of LAM on the cell surface or attachment of mycobacterial cells to the nitrocellulose membrane used in the initial screen. The absence of any obvious differences in CS-35 antibody binding as assessed by flow cytometry on both live and heat-killed wild-type and mutant strains favours the latter explanation.

Since the insertions in 7B7, 29D6 and 66C7 are close to the *pks15/1* gene implicated in PGL biosynthesis, we next investigated the production of PGL and related *p*-HBAD molecules in the mutants. As expected for a *M. tuberculosis* strain carrying the *pks15/1* mutation, the parent strain, Mt103, is devoid of PGL, but releases into the culture medium the mono- and tri-glycosylated *p*-Hydroxybenzoic acid methyl esters, *p*-HBAD-I and *p*-HBAD-II (Figs. 1 and 2). In addition, Mt103 secretes into the culture medium two other related glycoconjugates (Fig. 2). One of them was found to co-migrate with a rhamnosyl- α -*p*-hydroxybenzoic acid methyl ester standard and thus corresponds to an unmethylated form of *p*-HBAD-I (UM-*p*-HBAD-I) [21]. The second glycoconjugate (**G1**) migrating close to the origin (Fig. 2) was recently characterised as 2-*O*-methyl-fucosyl- α -(1 → 3)-rhamnosyl- α -(1 → 3)-2-*O*-methyl-rhamnosyl- α -*p*-hydroxybenzoic acid methyl ester, a truncated form of *p*-HBAD-II lacking two methyl groups on the fucosyl residue [21].

7B7, in contrast, secreted only the mono-glycosylated *p*-HBAD-I and UM-*p*-HBAD-I into the culture medium (Fig. 2). There was no evidence for the production of *p*-HBAD-II or related glycoconjugate **G1** in either the culture medium (Fig. 2) or in the bacterial cells of this mutant. Consistent with this observation, a recent publication [24] proposed that *Rv2958c* encodes the glycosyltransferase involved in the addition of the second rhamnosyl residue in *p*-HBAD-II and PGL (Fig. 1).

Unmethylated *p*-HBAD-I (UM-*p*-HBAD-I) was the only form of *p*-HBAD recovered from the culture filtrate of 29D6 (Fig. 2). This result is consistent with the recent characterisation of *Rv2959c* as the methyltransferase involved in the *O*-methylation of the hydroxyl group located at position 2 of the first rhamnosyl residue found in *p*-HBAD and PGL [25]. We recently reported the biochemical phenotype of 66C7 [21]. This mutant is totally deficient in the production of *p*-Hydroxybenzoic acid and consequently lacks all forms of *p*-hydroxybenzoate derivatives (Fig. 2). Further thin-layer chromatography analyses using a variety of solvents revealed no other qualitative or quantitative difference between the lipid contents of Mt103 and the mutants (data not shown).

3.3. Complementation of the mutants restores *p*-HBAD synthesis

7B7, 29D6 and 66C7 were complemented with wild-type copies of the *Rv2958c*, *Rv2959c* and *Rv2949c* genes respectively.

As described earlier, the complementation of 66C7 with plasmid pVVRv2949c restored the production of all forms of *p*-HBAD normally found in the wild-type strain [21].

Complementation of 7B7 restored both the production of *p*-HBAD-II and that of the partially methylated form of *p*-HBAD-II (**G1**) in the mutant (Fig. 2). However, probably due to the strong expression of *Rv2958c* in 7B7pVVRv2958c, all of the *p*-HBAD-I produced by the complemented strain was further glycosylated into *p*-HBAD-II, as no *p*-HBAD-I could be detected in the culture filtrates of 7B7pVVRv2958c. Interestingly, the complemented strain also accumulated a new glycoconjugate (**G2**), exhibiting a lower mobility than *p*-HBAD-II, which was not detected in the parent strain Mt103 (Fig. 2). This product was purified by preparative TLC and its native and derivatized forms were analyzed by a combination of MALDI-TOF mass spectrometry, GC, GC-MS and NMR as described in section 2.6. These analyses established that the most likely structure of compound **G2** is a tri-glycosylated form of *p*-HBAD in which the trisaccharide part consists of tri-*O*-methyl- α -L-Fucp-(1 → 3)- α -L-Rhap-(1 → 3)- α -L-Rhap (data not shown). It is likely that this product results from the direct glycosylation of UM-*p*-HBAD-I (without prior methylation), as a result of the over-expression of *Rv2958c* in the complemented strain.

Complementation of 29D6 with pVVRv2959c restored the synthesis of *p*-HBAD-I, *p*-HBAD-II and that of the glycoconjugate **G1** in the mutant, although the quantities of tri-glycosylated forms of *p*-HBAD (*p*-HBAD-II and **G1**) relative to *p*-HBAD-I were less than in the parent strain.

3.4. *p*-HBAD mutants show similar growth to the wild type strain in cultured macrophages and in mice

The growth rate of *M. tuberculosis* strains Mt103, 7B7, 29D6 and 66C7 in 7H9 broth was comparable (data not shown). Likewise, the mutants were found to grow similarly to the wild-type Mt103 in resting C57BL/6 bone marrow-derived macrophages (BMMs) over a 9-day period (Fig. 3). The ability of the wild-type and mutant strains to replicate and persist in the lung and spleen of C57BL/6 mice was then studied after intravenous infection of 10⁵ CFU. As shown on Fig. 4, the bacterial load in the spleens and lungs of mice infected with the mutants were comparable to those infected with the parent strain over 90 days.

3.5. *p*-HBAD mutants show histological differences in lung tissue of infected mice

In spite of bacillary loads remaining similar between all the strains, the pulmonary lesions induced by some of the mutants were significantly different from those induced by the parent strain. Forty-two days post-infection, while chronic lesions were observed in all groups of mice, the most severe lesions were observed with strain 7B7 (Fig. 5). The group of mice infected with this mutant showed diffuse and extensive lobular infiltrates containing large macrophages aggregated with lymphocytes. In addition to these symptoms of an acute inflammatory reaction, there was substantial local recruitment of polymorphonuclear cells as well as extensive and diffuse alveolitis extending to the pleural membrane. In comparison, the lesions induced by the wild-type strain Mt103 or by 29D6 displayed well-organised and mature granuloma-like structures containing large histiocytes associated with lymphocytes, with no extension to the pleural membrane, no or few polymorphonuclear cells and no vascular lesions (Fig. 5). 66C7-infected mice displayed an intermediate phenotype with a slightly more intense and diffuse inflammatory reaction than in Mt103-infected mice (Fig. 5). In agreement with the histological analysis, granuloma-like structures in the lungs of 7B7-, 66C7-, Mt103- and 29D6-infected mice 42 days post-infection occupied approximately 32, 27, 25 and 24% of histological sections, respectively.

3.6. Modulation of macrophage cytokine responses by p-HBAD mutants

To explore the mechanism by which the defects in the production of *p*-HBADs might contribute to the changes in gross histopathology of the lung, we compared pro-inflammatory cytokine production in C57BL/6 BMMs infected with Mt103 and each of the mutants. In all experiments, we confirmed that the number of phagocytosed bacteria was equivalent for all strains by plating CFU from additional control wells.

7B7 and 66C7 induced the secretion of significantly higher amounts of IL-6 and TNF α compared to Mt103 (Fig. 6) with typical increases of 2–2.5-fold for TNF α . 7B7 also caused a significant increase in IL-12 production (Fig. 6). 29D6 behaved similarly to Mt103.

Interestingly, the complemented mutant strain 7B7pVVRv2958c showed reversion of each of the cytokine profiles generated by 7B7 beyond that of the wild-type strain. This is likely due to the strong over-expression of *Rv2958c* in the complemented mutant, which directly affects the ratio of the tri-glycosylated forms of *p*-HBADs relative to the monoglycosylated forms (Fig. 2). Complementation of 66C7 with the wild-type copy of the *Rv2949c* gene restored the secretion of wild-type levels of IL-6 and TNF α (data not shown).

4. Discussion

The intriguing observation that most *M. tuberculosis* isolates fail to produce the virulence-associated PGL-tb while all strains analyzed to date have retained the ability to synthesize the glycosylated aromatic nucleus of these glycolipids, prompted us to study the role of *p*-HBADs in the pathogenesis of tuberculosis. To this end, the pathogenicity and immunogenicity of three mutants of *M. tuberculosis* Mt103 with defects in different aspects of *p*-HBAD synthesis were compared in macrophage and mouse models of infection.

None of the mutants, including 66C7, which is totally deficient in *p*-HBAD synthesis, showed any significant difference in growth in C57BL/6 mice and in macrophages compared to Mt103. However, there were appreciable differences in the lung histology of these mice. 7B7 and, to a lesser extent, 66C7 induced a significantly more severe and diffuse inflammation than Mt103. We conclude that the production of *p*-HBADs by *M. tuberculosis* strains has a significant impact on the host response to infection.

Our in vivo data suggest that this might initially be mediated through changes in the innate immune response of the host. Recognition of mycobacterial ligands by innate immune receptors on antigen-presenting cells results in activation of antimicrobial activities and release of cytokines that attract other immune cells and promote a Th1 adaptive immune response with production of IFN γ and increased macrophage activation. IL-6, IL-12 and TNF α are among the major cytokines required for pro-inflammatory responses, granuloma formation and development of a type 1 response during tuberculosis [26–28]. However, *M. tuberculosis* has evolved mechanisms to suppress this pathway permitting its survival and growth in macrophages [29]. The results of the present study demonstrated that failure to produce some or all forms of *p*-HBADs has the effect of reducing this suppression of innate immunity, thereby permitting increased production of IL-6, IL-12 and TNF α by macrophages.

The observation that our mutants differing solely in the carbohydrate moiety of these molecules induced different cytokine profiles suggests that at least some forms of *p*-HBADs do indeed play a role in this process. However, given the complex pattern and variable ratios of *p*-HBAD species secreted by the different strains analysed in the present study (Fig. 2), one cannot readily attribute a specific immunomodulatory activity to any given *p*-HBAD molecule. In the same way different types of PGL molecules induce different cytokine

responses by murine macrophages [3] it is likely that each different *p*-HBAD molecule, or strain-specific cocktail of *p*-HBAD molecules, causes distinct, even antagonist cytokine responses. Hence, the different cytokine levels observed upon infection of macrophages with the mutants reflect the overall response to the different *p*-HBADs cocktails generated by each individual strain.

A recent study suggested that the production of di- and tri-glycosylated *p*-HBADs conferred upon *M. tuberculosis* H37Rv an increased resistance to IFN γ -dependent but iNOS-independent immune antimicrobial pathways [30]. Our study suggests additional roles for *p*-HBADs in host infection and provides the first evidence that *p*-HBAD production by *M. tuberculosis* influences the release of key inflammatory cytokines by macrophages. We propose that the diminished ability of 66C7 and 7B7 to suppress the pro-inflammatory response results in severe pathology in the lungs of C57BL/6 mice due to the over-stimulation of the naturally strong basal immune response elicited by this strain of mouse. Next, it would be interesting to study the behaviour of the *p*-HBAD mutants in a mouse model exhibiting a less robust immune response to *M. tuberculosis* than C57Bl/6 mice. In a more susceptible mouse model, the anticipated enhanced stimulation of proinflammatory cytokines in response to the mutants may lead to improved control of infection and may reveal differences between the mutants in bacterial growth.

Acknowledgments

This work was supported by the European Commission, within the 5th and 6th Framework contract numbers; QLK2-CT-1999-01093 and LSHP-CT-2003-503367, the CONACyT fellowship no. 175523 from Mexico (to G. S.), the National Institutes of Health grant RO1 AI064798-01 (to M. J., R. G. and G. P.), the Marie Curie Training Site program no. CT-2000-00058 from the European Commission (to I. B.), the Medical Research Council and the Wellcome Trust and the Burroughs Wellcome Foundation, reference number 059125/Z/99/A. The text represents the authors' views and does not necessarily represent a position of the Commission who will not be liable for the use made of such information.

We thank scientists at Colorado State University (Fort Collins) for their kind provision of Mab CS-35 (in accordance with the NIH leprosy contract).

Abbreviations

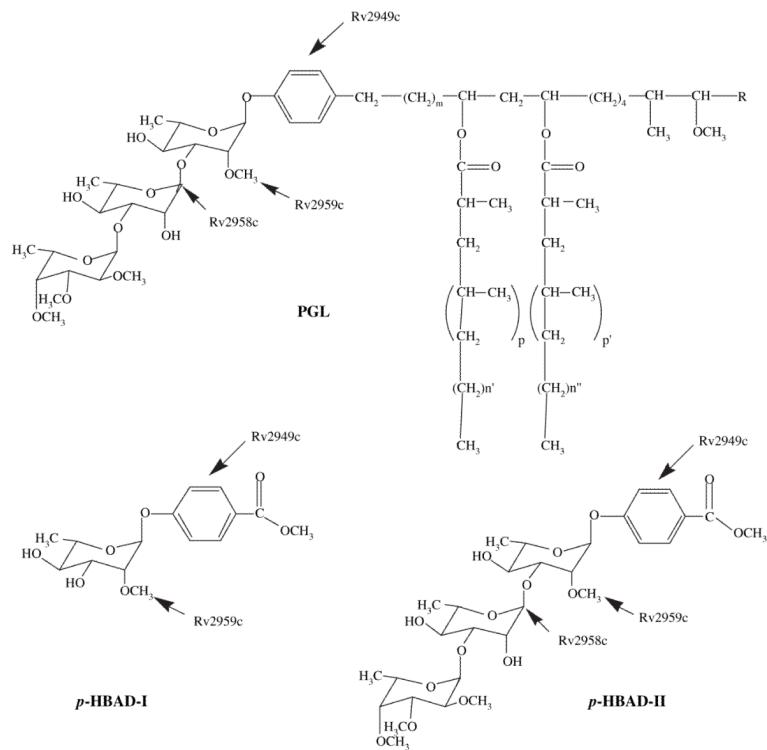
<i>p</i>-HBADs	<i>p</i> -Hydroxybenzoic acid derivatives
PGL	phenolic glycolipids

References

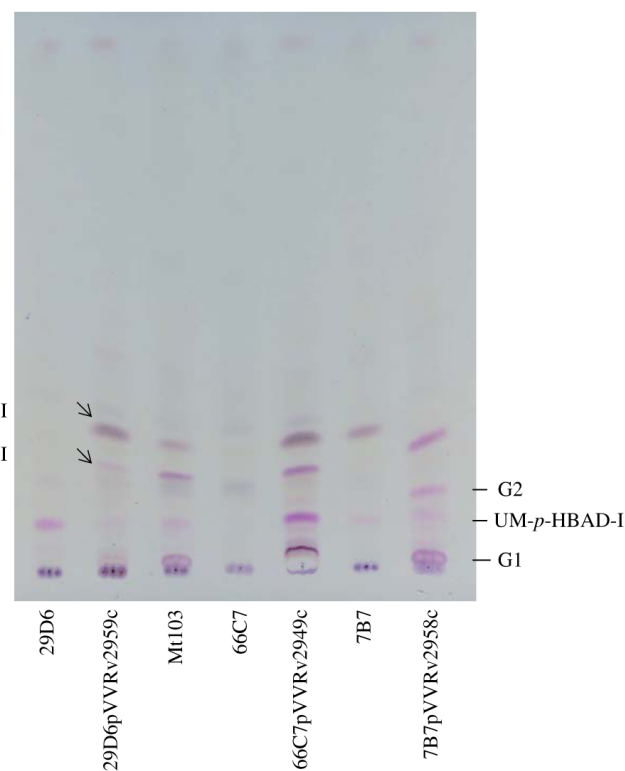
- [1]. Manca C, Tsenova L, Barry CE III, Bergtold A, Freeman S, Haslett PAJ, Musser JM, Freedman VH, Kaplan G. *Mycobacterium tuberculosis* CDC1551 induces a more vigorous host response in vivo and in vivo, but is not more virulent than other clinical isolates. *J. Immunol.* 1999; 162:6740–6746. [PubMed: 10352293]
- [2]. Rousseau C, Winter N, Pivert E, Bordat Y, Neyrolles O, Avé P, Huerre M, Gicquel B, Jackson M. Production of phthiocerol dimycocerosates protects *Mycobacterium tuberculosis* from the cidal activity of reactive nitrogen intermediates produced by macrophages and modulates the early immune response to infection. *Cell. Microbiol.* 2004; 6:277–287. [PubMed: 14764111]
- [3]. Reed MB, Domenech P, Manca C, Su H, Barczak AK, Kreiswirth BN, Kaplan G, Barry CE III. A glycolipid of hypervirulent tuberculosis strains that inhibits the innate immune response. *Nature.* 2004; 431:84–87. [PubMed: 15343336]
- [4]. Rao V, Fujiwara N, Porcelli SA, Glickman MS. *Mycobacterium tuberculosis* controls host innate immune activation through cyclopropane modification of a glycolipid effector molecule. *J. Exp. Med.* 2005; 201:535–543. [PubMed: 15710652]

- [5]. Tailleux L, Maeda N, Nigou J, Gicquel B, Neyrolles I. How is the phagocyte lectin keyboard played? Master class lesson by *Mycobacterium tuberculosis*. Trends Microbiol. 2003; 11:259–263. [PubMed: 12823942]
- [6]. Gatfield J, Pieters J. Molecular mechanisms of host-pathogen interaction: entry and survival of mycobacteria in macrophages. Adv. Immunol. 2003; 81:45–96. [PubMed: 14711053]
- [7]. Quesniaux V, Fremond C, Jacobs M, Parida S, Nicolle D, Yeremeev V, Bihl F, Erard F, Botha T, Drennan M, Soler M-N, Le Bert M, Schnyder B, Ryffel B. Toll-like receptor pathways in the immune responses to mycobacteria. Microbes Infect. 2004; 6:946–959. [PubMed: 15310472]
- [8]. Briken V, Porcelli SA, Besra GS, Kremer L. Mycobacterial lipoarabinomannan and related lipoglycans: from biogenesis to modulation of the immune response. Mol. Microbiol. 2004; 53:391–403. [PubMed: 15228522]
- [9]. Brennan, PJ. Microbial Lipids. Ratledge, C.; Wilkinson, SG., editors. Academic Press Ltd; London: 1988. p. 203–298.
- [10]. Puzo G. The carbohydrate- and lipid-containing cell wall of mycobacteria, phenolic glycolipids: structure and immunological properties. Critic. Rev. Microbiol. 1990; 17:305–327.
- [11]. Constant P, Pérez E, Malaga W, Lanéelle M-A, Saurel O, Daffé M, Guilhot C. Role of the *pks15/1* gene in the biosynthesis of phenolglycolipids in the *Mycobacterium tuberculosis* complex. J. Biol. Chem. 2002; 277:38148–38158. [PubMed: 12138124]
- [12]. Vachula M, Holzer TJ, Andersen BR. Suppression of monocyte oxidative response by phenolic glycolipid I of *Mycobacterium leprae*. J. Immunol. 1989; 60:203–206.
- [13]. Launois P, Blum L, Dieye A, Millan J, Sarthou JL, Bach MA. Phenolic glycolipid-I from *M. leprae* inhibits oxygen free radical production by human mononuclear cells. Res. Immunol. 1989; 140:847–855. [PubMed: 2697907]
- [14]. Vachula M, Holzer TJ, Kizlaitis L, Andersen BR. Effect of *Mycobacterium leprae*'s phenolic glycolipid-I on interferon-gamma augmentation of monocyte oxidative responses. Int. J. Lepr. Other Mycobact. Dis. 1990; 58:342–346. [PubMed: 2165510]
- [15]. Silva CL, Faccioli LH, Foss NT. Suppression of human monocyte cytokine release by phenolic glycolipid-I of *Mycobacterium leprae*. Int. J. Lepr. Other Mycob. Dis. 1993; 61:107–108.
- [16]. Charlab R, Sarno EN, Chatterjee D, Pessolani MC. Effect of unique *Mycobacterium leprae* phenolic glycolipid-I (PGL-I) on tumour necrosis factor production by human mononuclear cells. Lepr. Rev. 2001; 72:63–69. [PubMed: 11355520]
- [17]. Tsanova L, Ellison E, Harbacheuski R, Moreira AL, Kurepina N, Reed MB, Mathema B, Barry CE III, Kaplan G. Virulence of selected *Mycobacterium tuberculosis* clinical isolates in the rabbit model of meningitis is dependent on phenolic glycolipid produced by the bacilli. J. Infect. Dis. 2005; 192:98–106. [PubMed: 15942899]
- [18]. Jackson M, Raynaud C, Lanéelle M-A, Guilhot C, Laurent-Winter C, Ensergueix D, Gicquel B, Daffé M. Inactivation of the antigen 85C gene profoundly affects the mycolate content and alters the permeability of the *Mycobacterium tuberculosis* cell envelope. Mol. Microbiol. 1999; 31:1573–1587. [PubMed: 10200974]
- [19]. Hunter SW, Gaylord H, Brennan PJ. Structure and antigenicity of the phosphorylated lipopolysaccharide antigens from the leprosy and tubercle bacilli. J. Biol. Chem. 1986; 261:12345–12351. [PubMed: 3091602]
- [20]. Prod'hom G, Lagier B, Pelicic V, Hance AJ, Gicquel B, Guilhot C. A reliable amplification technique for the characterization of genomic DNA sequences flanking insertion sequences. FEMS Microbiol. Lett. 1998; 158:75–81. [PubMed: 9453159]
- [21]. Stadthagen G, Korduláková J, Griffin R, Constant P, Bottová I, Barilone N, Gicquel B, Daffé M, Jackson M. *p*-hydroxybenzoic acid synthesis in *Mycobacterium tuberculosis*. J. Biol. Chem. 2005; 280:40699–40706. [PubMed: 16210318]
- [22]. Nigou J, Gilleron M, Brando T, Puzo G. Structural analysis of mycobacterial lipoglycans. Appl. Biochem. Biotechnol. 2004; 118:253–267. [PubMed: 15304754]
- [23]. Jackson M, Phalen SW, Lagranderie M, Ensergueix D, Chavarot P, Marchal G, McMurray DN, Gicquel B, Guilhot C. Persistence and protective efficacy of a *Mycobacterium tuberculosis* auxotroph vaccine. Infect. Immun. 1999; 67:2867–2873. [PubMed: 10338493]

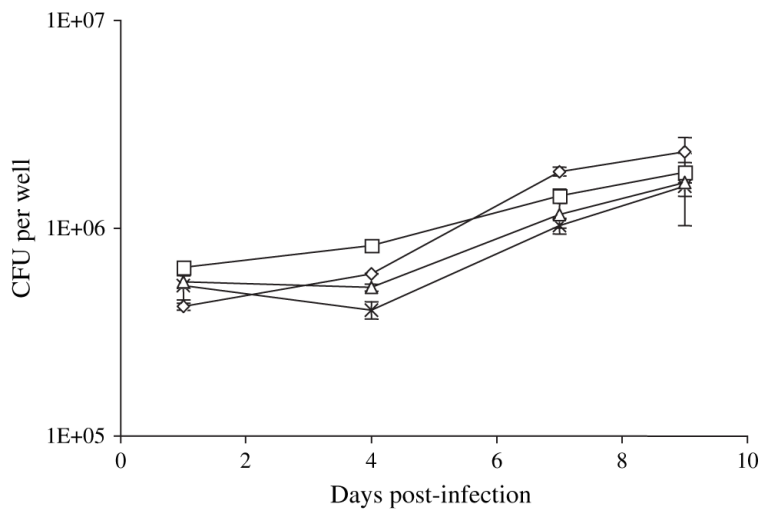
- [24]. Pérez E, Constant P, Lemassu A, Laval F, Daffé M, Guilhot C. Characterization of three glycosyltransferases involved in the biosynthesis of the phenolic glycolipid antigens from the *Mycobacterium tuberculosis* complex. *J. Biol. Chem.* 2004; 279:42574–42583. [PubMed: 15292272]
- [25]. Pérez E, Constant P, Laval F, Lemassu A, Lanéelle M-A, Daffé M, Guilhot C. Molecular dissection of the role of two methyltransferases in the biosynthesis of phenolglycolipids and phthiocerol dimycocerosate in the *Mycobacterium tuberculosis* complex. *J. Biol. Chem.* 2004; 279:42584–42592. [PubMed: 15292265]
- [26]. Orme, IM. Immunity to Mycobacterium. R.G. Landes Company; Texas, U.S.A.: 1995.
- [27]. Flynn JL, Chan J. Immunology of tuberculosis. *Annu. Rev. Immunol.* 2001; 19:93–129. [PubMed: 11244032]
- [28]. Kaufmann SH. How can immunology contribute to the control of tuberculosis? *Nat. Rev. Immunol.* 2001; 1:20–30. [PubMed: 11905811]
- [29]. Flynn JL, Chan J. Immune evasion by *Mycobacterium tuberculosis*: living with the enemy. *Curr. Opin. Immunol.* 2003; 15:450–455. [PubMed: 12900278]
- [30]. Hisert KB, Kirksey MA, Gomez JE, Sousa AO, Cox JS, Jacobs WR Jr, Nathan CF, McKinney JD. Identification of *Mycobacterium tuberculosis* counterimmune (*cim*) mutants in immunodeficient mice by differential screening. *Infect. Immun.* 2004; 72:5315–5321. [PubMed: 15322028]

**Fig. 1.**

Model structures of PGL, *p*-HBAD-I and *p*-HBAD-II from *M. tuberculosis*. The lipid core of PGL is composed of phenolphthiocerol esterified by mycocerosic acids ($m = 15-17$; $n = 20-22$, n' , $n'' = 16, 18$; $p, p' = 2-5$; $R = -CH_2-CH_3$ or $-CH_3$). The trisaccharide substituent, also found in *p*-HBAD-II, consists of 2,3,4-tri-*O*-methyl- α -L-Fucp-(1 \rightarrow 3)- α -L-Rhap-(1 \rightarrow 3)-2-*O*-methyl- α -L-Rhap. The monosaccharide substituent found in *p*-HBAD-I consists of 2-*O*-methyl- α -L-Rhap. The sites of action of the glycosyltransferase encoded by *Rv2958c*, of the methyltransferase encoded by *Rv2959c* and of the chorismate pyruvate-lyase encoded by *Rv2949c* are indicated by arrows.

**Fig. 2.**

Thin-layer chromatography analysis of lipids extracted from the culture supernatants of *M. tuberculosis* strains Mt103, 7B7, 29D6, 66C7 and the complemented mutant strains, 7B7pVVRv2958c, 29D6pVVRv2959c and 66C7pVVRv2949c. Equal volumes of lipid preparations extracted from the culture filtrates of each strain were applied to TLC plates, developed in CHCl₃/CH₃OH (95:5) and revealed with α -naphthol. The positions of *p*-HBAD-I, *p*-HBAD-II are indicated by arrows.

**Fig. 3.**

Growth of *M. tuberculosis* Mt103 and *p*-HBAD mutants in resting C57BL/6 bone-marrow-derived macrophages. The multiplicity of infection used is 1:10 bacterium per macrophage. The reported values represent the mean and standard deviation (error bars) of data obtained from three independent wells in one typical experiment. Wild-type Mt103 (diamonds); 7B7 (squares); 29D6 (crosses); 66C7 (triangles). Infection experiments were carried out in triplicate using three independent batches of bacterial preparations.

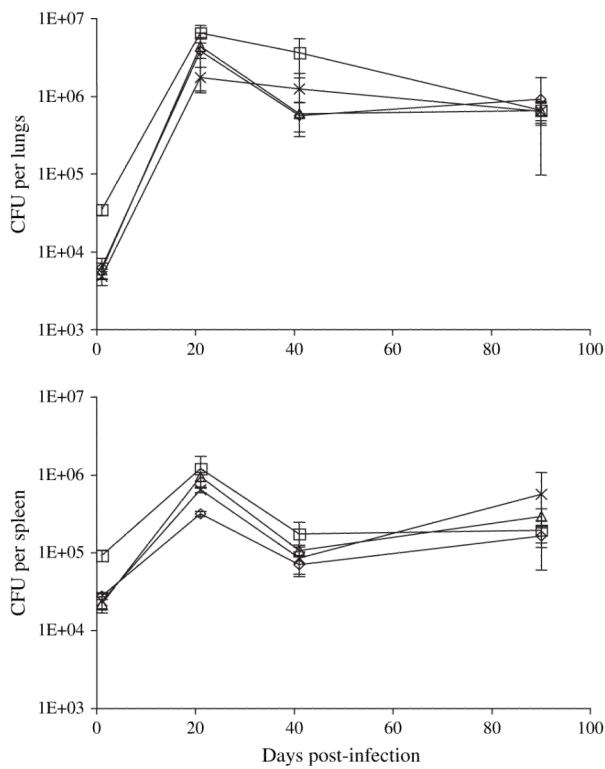
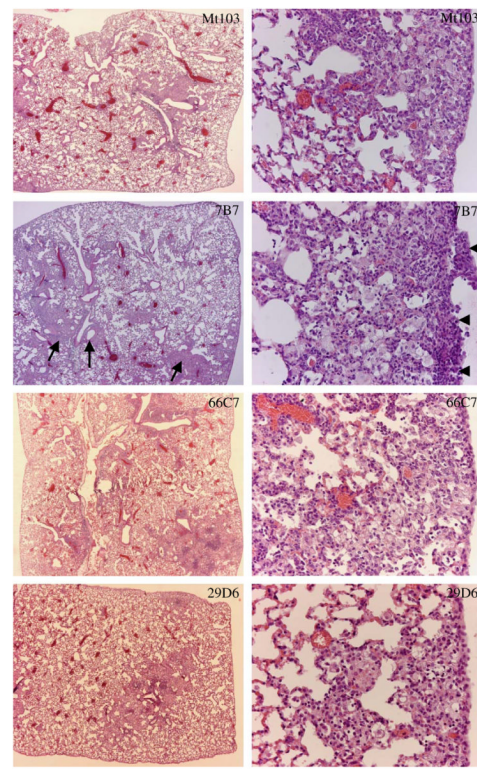
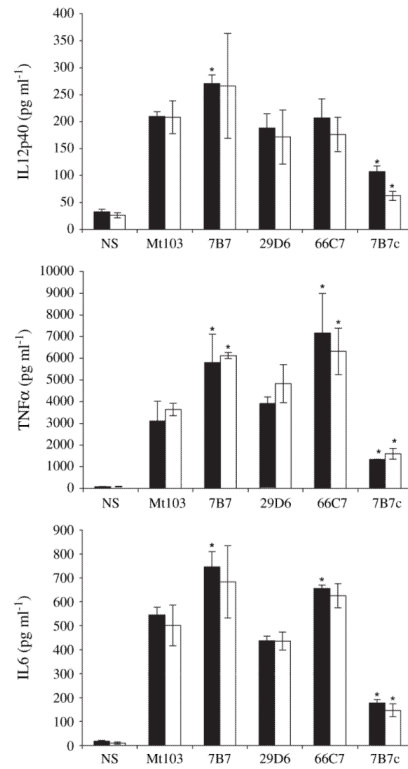


Fig. 4.
Multiplication and persistence of Mt103 wild-type and *p*-HBAD mutant strains in the lungs and spleen of intravenously-infected C57BL/6 mice. Results are expressed as means \pm standard deviations (error bars) of CFU counts for five infected mice. Wild-type Mt103 (diamonds); 7B7 (squares); 29D6 (crosses); 66C7 (triangles).

**Fig. 5.**

Typical pulmonary granuloma at 42 days post-infection from C57BL/6 mice infected with either *M. tuberculosis* Mt103, 7B7, 29D6 or 66C7. Sections were stained with hematoxylin and eosin. Left panels, magnification $\times 20$. Right panels, magnification $\times 200$. More lobular infiltrates (arrows) are seen in 7B7-infected mice with pleural effusion and numerous polymorphonuclear cells (arrowheads).

**Fig. 6.**

Cytokine secretion by C57BL/6 bone marrow-derived macrophages in response to infection with Mt103, 7B7, 29D6, 66C7 and 7B7 complemented strains. Supernatants of infected macrophages were assayed for the production of cytokines 24 (black bars) and 48 h (white bars) post-infection. Values represent the means \pm standard deviations (error bars) of cytokine production measured in three independent wells in one typical experiment. An asterisk indicates P values <0.05 (Student's t test) for the comparison of wild-type *vs* mutant strains. Cytokine production was measured in three independent experiments using fresh cell and bacterial preparations.

Table 1

Location of transposon and predicted function of disrupted genes in 25 transposon mutants of *M. tuberculosis*, including the three strains investigated in this study

Mutant designation	<i>M. tuberculosis</i> H37Rv Gene ID	Position of insertion ^a	Gene function
7B7	Rv2958c	-17 bp	Glycosyltransferase
29D6	Rv2959c	+666 bp	Methyltransferase
66C7	Rv2949c	+237 bp	Chorismate pyruvate-lyase
43G6	Rv1502	+657 bp	Unknown; close to several glycosyltransferase genes
18G7	Rv0193c	+392 bp	Unknown
25E7	Rv1948c	+32 bp	Unknown
5C2	Rv2020c	+295 bp	Unknown
23D4	intergenic region in RvD2	-	Unknown
41F5	Rv3480c	-54 bp	Unknown
44B5	Rv2387	-297 bp	Unknown
34D6	Rv2338c (<i>moeW</i>)	+920 bp	Possible molybdopterin biosynthesis protein
33G4	Rv2338c (<i>moeW</i>)	+383 bp	Possible molybdopterin biosynthesis protein
7H10	Rv2339 (<i>mmpL9</i>)	+311 bp	Probable transmembrane transport protein
41E5	Rv2339 (<i>mmpL9</i>)	+1542 bp	Probable transmembrane transport protein
28H4	Rv0987	+1592 bp	Probable transmembrane protein ABC transporter
3A10	Rv3500c (<i>yrbE4B</i>)	+605 bp	Membrane protein
3F7	Rv0304c (<i>ppe5</i>)	+6598 bp	PPE family protein
2G7	Rv3343c (<i>ppe54</i>)	+2594 bp	PPE family protein
35D3	Rv1548c (<i>ppe21</i>)	+1073 bp	PPE family protein
31D7	Rv0112 (<i>gca</i>)	+329 bp	Possible GDP-mannose 4, 6 dehydratase
20H5	Rv0449c	+520 bp	Putative dehydrogenase
24F7	Rv0456c (<i>echA2</i>)	-700 bp	<i>echA2</i> , enoyl-CoA hydratase;
59D7	Rv1664 (<i>pks9</i>)	+3017 bp	Unknown polyketide synthase
34B8	Rv3825c (<i>pks2</i>)	+3213 bp	Polyketide synthase (sulfolipid synthesis)
35B10	Rv2368c	+568 bp	Probable PhoH-like protein

^aPosition of insertion relative to the predicted start codon of the gene (<http://genolist.pasteur.fr/TubercuList/>). Negative values indicate that the transposon is inserted in an intergenic region upstream from the start codon of the indicated gene.